

ANNUAL SIMULATIONS OF HEAT PUMP SYSTEMS WITH VERTICAL GROUND HEAT EXCHANGERS

Michel A. Bernier Duo Randriamiarinjatovo
École Polytechnique de Montréal
Département de génie mécanique
mibern@meca.polymtl.ca rduo@meca.polymtl.ca

ABSTRACT

This article presents a methodology that has been developed to perform annual hour-by-hour simulations of a single zone building heated/cooled by water source heat pumps coupled to a vertical ground heat exchanger.

The computer program simulates the three distinct parts of the system: i) building load; ii) heat pump; iii) and ground heat exchanger. The coupled governing equations of these three models are solved simultaneously until a converged solution is obtained at each time step. Simulations are performed using a commercially-available equation solver called EES.

Results of annual simulations are presented. It is shown that the program can be useful to balance ground heat exchanger length against heat pump energy consumption.

INTRODUCTION

Ground-coupled heat pump (GCHP) systems are becoming increasingly popular because of their energy saving potential. The system under study is presented in figure 1. It consists of a single-zone building with one heat pump, a circulating pump and a vertical ground heat exchanger. As shown in figure 1, a vertical GCHP system is usually composed of a series of boreholes (only one is shown on figure 1). After its passage through the heat pump, a certain amount of heat, identified as " q " in figure 1, is released into the loop to the circulating fluid. The fluid enters the ground at a temperature $T_{out,HP}$. Heat is then exchanged, at a rate equal to q , between this fluid and the surrounding ground. The fluid leaves the borefield at a temperature $T_{in,HP}$.

The rate at which heat is exchanged in the ground will depend on the temperature level which, in turn, depends on heat pump performance. Thus, heat pump performance and ground heat transfer are coupled via the temperature in the loop.

The economic decision to select a GCHP system for a particular application is most often dictated by the length of the ground heat exchanger and by energy saving potential offered by GCHP systems. An undersized heat exchanger will lead to unacceptably low (high) inlet temperatures in the winter (summer) months. An oversized heat exchanger, on the other hand, while providing safe heat pump operation, may lead to prohibitive installation costs.

This article presents a method to perform annual simulations of GCHP systems which can be used to optimise the length of the ground heat exchanger and provide annual energy consumption.

CURRENT METHODS

Ground heat exchanger sizing

There are several methods of sizing vertical ground heat exchangers. These methods have been reviewed and compared by Shonder et al. (1999, 2000). In essence, they use precalculated peak heating and cooling loads and average monthly building loads. The building loads are converted to ground loads using given values of COP and EER (which, in some sizing programs, are constant throughout the year). Then, the length required in heating and cooling is estimated using these ground loads in conjunction with the minimum and maximum entering water temperatures. The length estimation is based on ground heat exchanger models which use different methods to handle transient heat transfer in the ground. Models based on the cylindrical heat source method (e.g. Kavanaugh and Rafferty, 1997 and Bernier, 2000, Morrison, 2000) and the g-function (Yavuzturk and Spitler, 1999) are available.

The main characteristics of these approaches is that the building load is decoupled from the ground. In other words, loads and ground heat transfer are treated sequentially with no interaction between the two.

Whole system simulations

To our knowledge there are only two simulation programs that can perform annual simulations of a complete GCHP system including building load

interactions. The first of these programs is DOE. As reported by McLain and Martin (1999), DOE-2.1E has a subroutine to handle ground heat transfer. However, its performance seems to be relatively poor when compared to experimental data.

The second simulation program is TRNSYS coupled with the DST model of the University of Lund (Hellström et al., 1996). There is a general consensus in the GCHP research community that the DST-TRNSYS combination is probably the best available to perform whole system simulation. However, based on our own experience the TRNSYS environment is difficult to learn (Bernier, 1999).

This paper presents a methodology to perform accurate simulations of complete systems in a user-friendly environment. The building load, ground heat transfer, and heat pump performance are calculated simultaneously at each time step.

METHODOLOGY

Building load calculations

The load calculation portion of the proposed approach accounts for heat transfer through opaque surfaces; solar heat gains and conductive gains/losses through windows; and internal heat gains.

Heat transfer through opaque surfaces. There are six opaque surfaces in the monozone building used here. The four walls are assumed to be identical while the roof and the floor have different configurations. As shown in figure 2, it is possible to specify up to three different layers in the walls, as well as in the roof and floor. Assuming one-dimensional heat flow, transient heat transfer in the opaque surfaces is governed by :

$$\rho C_p \frac{\partial T}{\partial t} = \frac{\partial}{\partial x} \left(k \frac{\partial T}{\partial x} \right) \quad (1)$$

where ρ is the density (kg/m^3), C_p is the specific heat (J/kg-K), k is the thermal conductivity (W/m-K), t is the time (sec), x is the position in the wall (m), and T is the temperature ($^{\circ}\text{C}$).

The boundary conditions are also shown on figure 2. The interior temperature, T_{int} , as well as the temperature in the adjacent room, T_{adj} , are assumed constant throughout the year. Exterior temperature and solar radiation vary on an hourly basis. These last two parameters are combined using the concept of sol-air temperature (ASHRAE, 1997).

The value of $q_{ext,i}$ (Figure 2) is then given by:

$$q_{ext,i} = h_o (T_{sol-air,i} - T_{s,ext,i}) \quad (2)$$

where,

$T_{sol-air,i}$ is the sol-air temperature for surface "i"; h_o is the outside film coefficient (this coefficient is assumed constant and equal to $16.94 \text{ W/m}^2\text{-K}$); $T_{s,ext,i}$ is the external surface temperature for surface "i" .

Convective heat exchanges on internal surfaces are given by:

$$q_{conv,in,i} = h_{conv,i} (T_{int} - T_{s,int,i}) \quad (3)$$

where $T_{s,int,i}$ is the internal surface temperature of surface "i" and $h_{conv,i}$ is the convective film coefficient. The terms associated with long-wave radiation, $q_{lw,i}$, represents the sum of two terms:

$$q_{lw,i} = q_{lw,surf,i} + q_{lw,gains} \quad (4)$$

where $q_{lw,surf,i}$ is the net long-wave radiation incident on surface i coming from the other five surfaces and $q_{lw,gains}$ is the incident long-wave radiation received from the radiative portion of the internal gains. In this work, it is assumed that the radiative portion of the internal gains is equally distributed among all six surfaces. The values of $q_{lw,surf,i}$ are obtained by solving:

$$q_{lw,surf,i} = \frac{Eb_i - J_i}{1 - \epsilon_i} \quad (5)$$

$$q_{lw,surf,i} = \frac{\sum_{k=1}^6 \frac{J_i - J_k}{1 - \epsilon_i}}{A_i F_{i,k}} \quad \text{for } i = 1 \text{ to } 6$$

where Eb_i is the emissive power ($\sigma T_{s,int,i}^4$), J represents radiosity, A_i is the surface area, $F_{i,k}$ is the form factor between surface i and k , and ϵ_i is the emissivity of surface "i".

The last boundary condition is $q_{solar,f}$. It is the amount of solar energy transmitted through the window and intercepted by the floor. It is assumed here that all of the solar energy transmitted through the windows is absorbed evenly by the floor. Consequently, $q_{solar,f}$ is given by:

$$q_{solar,f} = \sum_{i=2}^5 G_{t,i} \times \tau_i \times \frac{A_{window,i}}{A_{floor}} \quad (6)$$

where the summation extends from $i=2$ (south wall) to $i=5$ (east wall) and τ_i is the solar transmittance of window "i". Incident solar radiation on each surface, $G_{t,i}$, is calculated using:

$$G_t = G_{ND} \cos \theta + G_{dH} \frac{(1 + \cos \beta)}{2} + \rho G_{tH} \frac{(1 - \cos \beta)}{2} \quad (7)$$

where G_{IH} is the total horizontal radiation, G_{DN} is the direct normal radiation, and G_{dH} is the diffuse radiation on the horizontal. These three values of solar radiation are obtained from meteorological data files. The angle between the normal to the surface and the solar rays is θ while β is the slope (from horizontal) of the surface and ρ is the albedo.

To summarise, equation 1 is the governing equation to be solved and the boundary conditions are given by equations 2,3,4,5,and 6 . This problem is solved using the control-volume approach proposed by Patankar (1980). With reference to figure 3, the fully implicit form of the discretization equation for an internal node is given by :

$$a_P T_P = a_E T_E + a_O T_O + b \quad (8)$$

where

$$a_P = a_E + a_O + a_P^0, \quad a_E = \frac{k_e}{\delta x_e}, \quad a_O = \frac{k_o}{\delta x_o},$$

$$\text{and } a_P^0 = \frac{\rho C_p \Delta x}{\Delta t}, \quad b = a_P^0 T_P^0$$

Δx is the width of the control volume, T_P^0 is the temperature at point P prevailing at the preceding time interval, k_e and k_o are so-called interface conductivities which account for different thermal conductivities between adjacent nodes (Patankar,1980). With this approach, sudden changes in the value of k can be handled even with a coarse mesh near the interface.

Boundary nodes require a special treatment. Taking the floor surface temperature as an example ($T_{s,int,f}$ in figure 2 and node B in figure 3), the values of a_B^0 and b are given by:

$$a_B^0 = \frac{\rho C_p (\Delta x/2)}{\Delta t},$$

$$b = a_B^0 T_B^0 + q_{hw,f} + q_{conv,f} + q_{solar,f} \quad (9)$$

As indicated in figure 3, nine grid points, three in each layer, were selected. This grid spacing is the result of a compromise between accuracy and calculation speed. Figure 4 presents the result of a comparison between the TFM method (ASHRAE,1997) and the method used here with 9 and 15 grid points. These results show that there is good agreement between the three sets of results. The 15 grid points solution is closer to the TFM solution than the 9 grid point solution. However, a 9 grid point spacing was retained to reduce calculation time. Finally, it should be noted that over a 24 hour

period, the average value of $q_{conv,in,i}$ obtained with 9 grid points and the TFM method agree within 1%.

Internal heat gains. The treatment of internal heat gains, q_{gains} , is relatively straightforward. The convective portion of the internal gains, which contributes immediately to the heating/cooling load is given by:

$$q_{gains,conv} = F_{conv} \times q_{gains} \quad (10)$$

where F_{conv} is the convective fraction of internal heat gains. The radiative portion of the heat gains, $q_{gain,rad}$, is simply given by:

$$q_{gains,rad} = q_{gains} - q_{gains,conv} \quad (11)$$

Solar heat gains through windows. As indicated earlier in conjunction with equation 7, the amount of solar energy that enters the room, $q_{solar,in}$ is given by:

$$q_{solar,in} = \sum_{i=2}^5 G_{t,i} \times \tau_i \times A_{window,i} \quad (12)$$

Convective heat gains/losses through windows. These gains/losses are evaluated simply by solving:

$$q_{conv,window} = \sum_{i=2}^5 U_i \times A_{window,i} \times (T_{ext} - T_{int}) \quad (13)$$

where U_i is the heat loss coefficient of window "i".

Calculation of the heating/cooling load. Equations 1 to 13 are solved simultaneously until a converged solution is obtained. The heating/cooling load is then obtained by:

$$q_{load} = \sum_{i=1}^6 q_{conv,in,i} + q_{gains,conv} + q_{conv,window} \quad (14)$$

Ground loop calculations

Figure 5 presents the main components of a vertical ground heat exchanger. This figure is in fact an input screen extracted from the software. The left portion of the figure shows the borefield arrangement. In this case there are a total of 4 boreholes, arranged in a 2x2 grid. Their center-to-center distance is 6 m and the total length of the loop is 75 m. The initial ground temperature is 10°C. The right portion of the figure shows the internal configuration of the borehole. It consists of two tubes separated by a certain distance and located away from the borehole wall (configuration "B" of Remund, 1997). The borehole is filled with a grout whose thermal properties might be different from the ones of the adjoining soil.

The characteristics that are needed to define transient heat transfer in the ground are presented on the right portion of the figure. From top to bottom, these

characteristics are: soil thermal diffusivity (α_s), soil thermal conductivity (k_s), grout thermal conductivity (k_g), borehole diameter, pipe internal and external diameters and thermal conductivity (k_p).

Transient heat transfer in the ground is similar to transient heat transfer in a wall in that energy storage, or the "thermal history" as to be accounted for. However, in the case of ground heat transfer, the thermal history as to be kept relatively long. Computationally, this complicates calculations. In the approach proposed in this paper, transient heat transfer in the ground is calculated using the cylindrical heat source method with a load aggregation scheme which reduces computational time. This method will now be described briefly. The readers are referred to other publications (e.g. Kavanaugh and Rafferty, 1997 and Bernier, 2001) for a more complete description of the method.

With reference to figure 6, the mean fluid temperature in the borefield at time n, referred here as $T_{f,n}$, is given by:

$$T_{f,n} = \frac{q_n}{L} R_b - \frac{1}{k_s L} \left[q_{mean,m} (G_{Fo_{n,0}} - G_{Fo_{n,t_m}}) + q_{m+1} (G_{Fo_{n,t_m}} - G_{Fo_{n,t_{m+1}}}) + q_{m+2} (G_{Fo_{n,t_{m+1}}} - G_{Fo_{n,t_{m+2}}}) + \dots + q_n (G_{Fo_{n,t_{m+A-1}}}) \right] - T_{g,n} \quad (15)$$

where,

q_n is the heat transfer rate during the last time interval, from t_{m+A-1} to t_n , (Watts). A positive value of "q" implies heating, i.e. heat transfer from the ground to the fluid; R_b is the effective borehole thermal resistance, (m-K/W); L is the total length of the boreholes (not to be confused with the pipe length which is twice the borehole length), (m); $q_{mean,m}$ is the aggregated load, i.e. the average heat transfer rate during the time interval from 0 to t_m , (Watts); $A (= t_n - t_m)$ is the "short term thermal history" time interval, (hours); $T_{g,n}$ is the far field ground temperature at time n.

The "G" function requires some further discussion. As shown in equation 15, this function is evaluated for a given Fourier number, Fo, which is defined by:

$$Fo = 4\alpha_s t / d^2 \quad (16)$$

where,

t is the time (in days) and d is the borehole diameter (m). The "G" function is in fact the analytical solution to transient heat transfer (Ingersoll et al., 1954) from a cylinder embedded in an infinite medium subjected to a

constant heat transfer rate. The ratio G_{Fo}/k_s represents an effective thermal resistance. The "G" function is relatively complex. In this work, the curve fitted expression suggested by Bernier (2001) has been used.

Equation 15 reflects the use of the principle of superposition to accommodate variable heat transfer rates. For example, the term associated with q_{m+1} represents the contribution of q_{m+1} to the final value of $T_{f,n}$. It is calculated by assuming that q_{m+1} prevails over the time interval from t_m to t_n from which is subtracted the superimposed effect of q_{m+1} over the time interval from t_{m+1} to t_n .

Recognising that the immediate short term thermal history is more important than the past thermal history in the determination of $T_{f,n}$, the past thermal history is averaged into a single term while the short term thermal history is kept intact. Yavuzturk and Spitler (1999) have referred to this as "load aggregation". This technique is illustrated schematically in figure 6 with an example of a calculation performed at hour 5168 and where the short term thermal history consists of the last 168 hours prior to hour 5168. By using load aggregation, equation 15 contains 169 terms (instead of 5168 terms if load aggregation was not used) with the impact of the first 5000 hours combined into a single term, $q_{mean,m}$.

The first term on the right hand side of equation 15 represents heat transfer from the fluid to the wall of the borehole. It is assumed that this process occurs in steady state and that it can be described using an equivalent borehole thermal resistance, R_b , based on the concept of shape factors (Remund 1999).

When a borefield is composed of several boreholes, heat gets stored (retrieved) between boreholes, thereby increasing (decreasing) the value of T_g . Kavanaugh and Rafferty (1997) have proposed a correction procedure that was used in the present approach. The readers are referred to the book by Kavanaugh and Rafferty for more details.

To summarise, equation 15 is the main governing equation to evaluate ground heat transfer. It calculates the mean fluid temperature in the borefield at time t_n . It accounts for two groups of heat transfer rates. The first one is associated with the immediate thermal history, i.e. interval A in figure 6. The second heat transfer rate is an aggregated load that covers the time period prior to the immediate thermal history.

Ground loop calculations using equation 15 have been validated successfully against the DST model. Results are presented in a related paper (Bernier, 2001).

Heat pump performance

Heat pump performance depends mainly on four factors: room air temperature, air flow rate, water flow rate, and entering water temperature. Generally, the first three factors are fixed by design and only the entering water temperature varies during the course of a year.

In this work, heat pump performance, characterised by the Coefficient of Performance (COP), is calculated using "lookup tables". One such table is presented in figure 7 for both heating and cooling. These tables are generated by entering catalogue data.

During calculations, the operating COP is evaluated at the entering water temperature based on a linear interpolation between values contained in the lookup tables. Once the COP is known, the amount of heat rejected (HR) (or the amount of heat extracted (HE), if the building is in cooling mode), and the heat pump energy consumption (EC_{HP}) are calculated using:

$$HR = q_{load} \times \left[1 + \frac{1}{COP_{cooling}} \right] \quad (17)$$

$$HE = q_{load} \times \left[1 - \frac{1}{COP_{heating}} \right] \quad (18)$$

$$EC_{hp} = \left| \frac{q_{load}}{COP_{cooling \text{ or } heating}} \right| \quad (19)$$

SOFTWARE IMPLEMENTATION

The equations described in this paper were implemented in a commercially-available solver called EES which stands for Engineering Equation Solver (Klein, 2000). One of the nicest feature of this solver is the diagram window capability which makes entering data very user-friendly. One such graphic is presented in figure 5.

EES uses a variant of Newton's method to solve the set of non-linear algebraic equations. The Jacobian matrix is evaluated at each iteration. Blocking algorithm and sparse matrix techniques are used to break the problem into smaller problems and improve calculation efficiency.

Since the governing equations of ground heat transfer and heat pump performance are coupled, an iterative solution procedure is needed. In a nutshell, the iteration procedure assumes different values of $T_{in,HP}$ until the amount of energy rejected into the loop is equal to the amount of energy released into the ground.

RESULTS

Simulations are performed for a 3×3×3 m single-zone building located in Montréal and maintained at 24°C all year round. The four walls are facing the four cardinal points and each has a 4 m² window. Using the building material terminology of ASHRAE (page 28.19 of the ASHRAE Handbook of Fundamentals, 1997), the construction of the building envelope is the following:

Window: $U=3.3 \text{ W/m}^2\text{-K}$, $\tau = 0.8$

Walls: A2-B16-E1

Roof: B7-B16-E1

Floor: E1-C12-E13

with $h_o = 16.94 \text{ W/m}^2\text{-K}$ and $h_{conv,i} = 3.4 \text{ W/m}^2\text{-K}$. All surfaces are assumed to have an emissivity of 0.9.

Internal heat gains are assumed constant and equal to 2500 W with a convection/radiation split of 50/50.

The borefield arrangement as well as the ground properties are shown in figure 5. The heat pump COP is given in figure 7 for both heating and cooling. The flow rate is set at 0.24 L/sec. Finally, ground heat exchanger simulations were performed with a 24 hour load aggregation period.

Figure 8 shows the resulting building loads. The peak loads are -3.6 kW in heating and 4.8 kW in cooling. At this point, if current sizing methods are used, the length determination of the ground heat exchanger would proceed by estimating ground loads based on an average annual COP. Using the data of figure 8 and based on an average annual COP of 3.5, it can be shown that: i) the average power (on a yearly basis) released into the ground is 270 W (a positive ground load means that heat is being transferred from the ground to the circulating fluid); ii) the average monthly power rejected/absorbed into the ground is -1.9kW/+1.7kW for the most severe months (July/January); iii) the maximum hourly heat rejection into the ground occurs in July and is equal to -6.2 kW. In January, the ground provides +2.6 kW of heat to the heat pumps. Using these values and the ground properties indicated in figure 5 in a sizing program (Bernier, 2000), it can be shown that the required heating length is 95 m while the required cooling length is 79 m. These lengths are based on maximum entering water temperatures of +1.5°C and +32.5°C in heating and cooling, respectively.

Figure 9 presents the results of annual hour-by-hour simulations for two different heat exchanger lengths, 75 and 67.5 m. Both graphs show the variation of the inlet

temperatures to the heat pumps. As shown on the left graph, a heat exchanger length of 75m is adequate to remain within the lower and upper temperatures used in the sizing procedure described above. Thus, in this particular case, the heat exchanger length estimation is lower when using annual simulations. This is due to the fact that hour-by-hour simulations can "follow" the ground loads more precisely while current sizing procedure are based on the maximum hourly, monthly, and yearly thermal pulses.

The other main advantage of hour-by-hour simulations is that heat pump energy consumption can be calculated precisely using hourly values of COP. For instance, with a 75m heat exchanger, annual heat pump energy consumption is 3300 kWh. The graph on the right of figure 9 shows the impact of a 10% reduction (from 75m to 67.5m) in heat exchanger length on T_{inHP} and annual heat pump energy consumption. The lower and upper limits of T_{inHP} are lower/higher than for the case where the length is 75m. In fact, temperatures of -1.6°C and 39°C are dangerously close to the safe operation limit of heat pumps. In addition, results in Figure 9 show that heat pump energy consumption increases by 6% due to lower COP values attributable to lower/higher values of T_{inHP} in heating/cooling.

CONCLUDING REMARKS

A methodology has been presented to solve simultaneously the coupled governing equations of building load, heat pump performance, and ground heat transfer. These equations are solved using a commercially-available equation solver called EES.

Hourly simulations for a complete year are presented for a 27m^3 cube subjected to Montréal weather conditions. This room is coupled to a 75m vertical ground heat exchanger and heated/cooled by a single heat pump. Results show that the proposed methodology has the advantage of giving a more precise estimate of heat exchanger length when compared to current sizing procedures. Furthermore, heat pump energy consumption can be calculated more accurately since hourly COP values, obtained from predictions of the outlet ground temperature, are used.

REFERENCES

ASHRAE. (1997). *ASHRAE Handbook of Fundamentals*,ASHRAE.

Bernier, M.A. (1999). L'apprentissage de TRNSYS/IIiSiBat par des étudiants en génie climatique, 2^{ième} séminaire TRNSYS francophone, 12 pages, Montréal,.

Bernier M. (2001). Ground-Coupled Heat Pump System Simulation, *ASHRAE Transactions* 107 (1).

Bernier, M. (2000). A Review of the Cylindrical Heat Source Method for the Design and Analysis of Vertical Ground-Coupled Heat Pump Systems. 4th International Conference on Heat Pumps in Cold Climate, Aylmer, Québec.

Hellström, G., Mazzarella, L., Pahud,D. (1996). Duct ground storage model – TRNSYS version. Department of Mathematical Physics, University Of Lund, Sweden.

Ingersoll, L.R., Zobel, O.J., Ingersoll, A.C. (1954). *Heat Conduction With Engineering, Geological, And Other Applications*, University Of Wisconsin Press.

Kavanaugh S.P., Rafferty, K. (1997). *Ground-Source Heat Pumps : Design Of Geothermal Systems For Commercial And Institutional Buildings*. ASHRAE, Atlanta, GA.

Klein, S.A. (2000). *EES – Engineering Equation Solver*, F-chart software, Madison, Wisconsin.

McLain, H.A., Martin, M.A., (1999). A Preliminary Evaluation of the DOE-2.1E Ground Vertical Well Model Using Maxey School Measured Data. *ASHRAE Transactions*, 105 (2).

Morrison, A. (2000). GS2000TM software, 4th International Conference on Heat Pumps in Cold Climate, Aylmer, Québec.

Patankar, S.V., (1980). *Numerical Heat Transfer and Fluid Flow*, McGraw-Hill.

Remund, C.P. (1999). Borehole Thermal Resistance : Laboratory and Field Studies, *ASHRAE Transactions* 105 (1) : 439-445.

Shonder, J.A., Baxter, V., Thornton, J., Hughes, P., (1999). A New Comparison Of Vertical Ground Heat Exchanger Design Methods For Residential Applications. *ASHRAE Transactions*, 105 (2).

Shonder, J.A., Baxter, V.D., Hughes, P.J., Thornton, J.W., (2000). A Comparison of Vertical Ground Heat Exchanger Design Software for Commercial Applications, *ASHRAE Transactions* 106 (1).

Yavuzturk, C., Spitler, J.D., Rees, S.J. (1999). A Transient Two-Dimensional Finite Volume Model For the Simulation of Vertical U-Tube Ground Heat Exchangers, *ASHRAE Transactions* 105 (2).

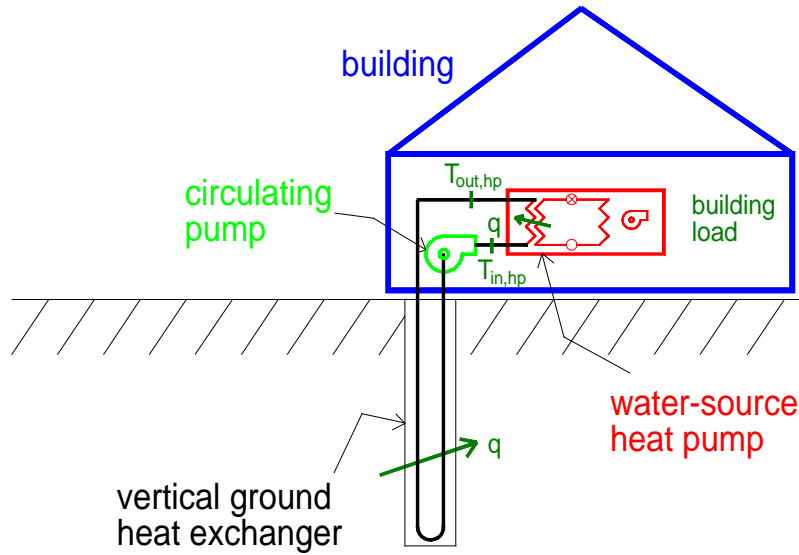


Figure 1. Schematic representation of the problem under study.

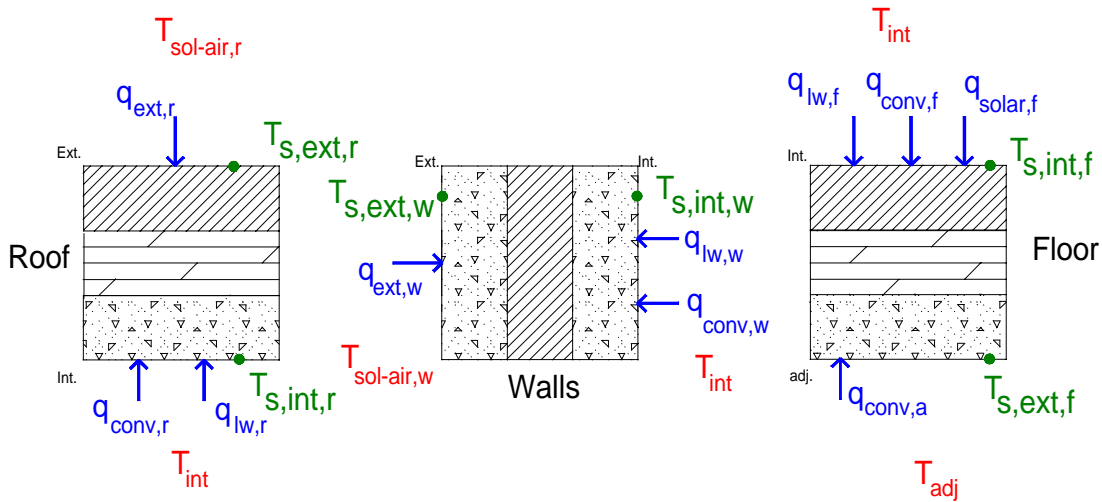


Figure 2. Nomenclature used to describe heat transfer through the walls, the roof, and the floor.

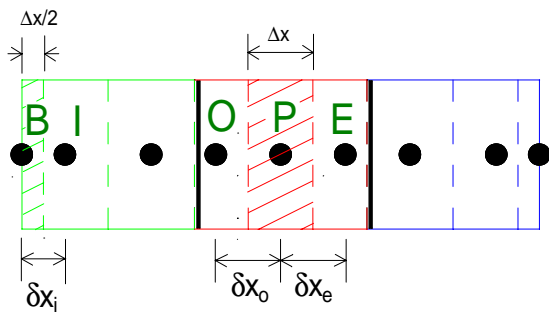


Figure 3. Grid arrangement for a three layer opaque surface.

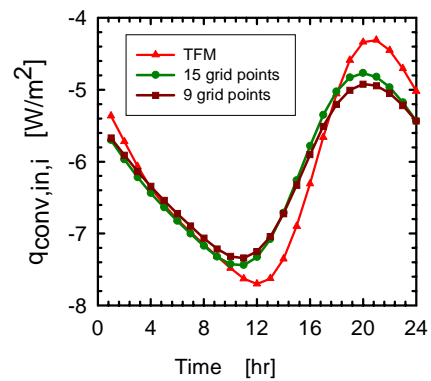


Figure 4. Heat transfer at the internal surface. Comparison between the TFM and the proposed method.

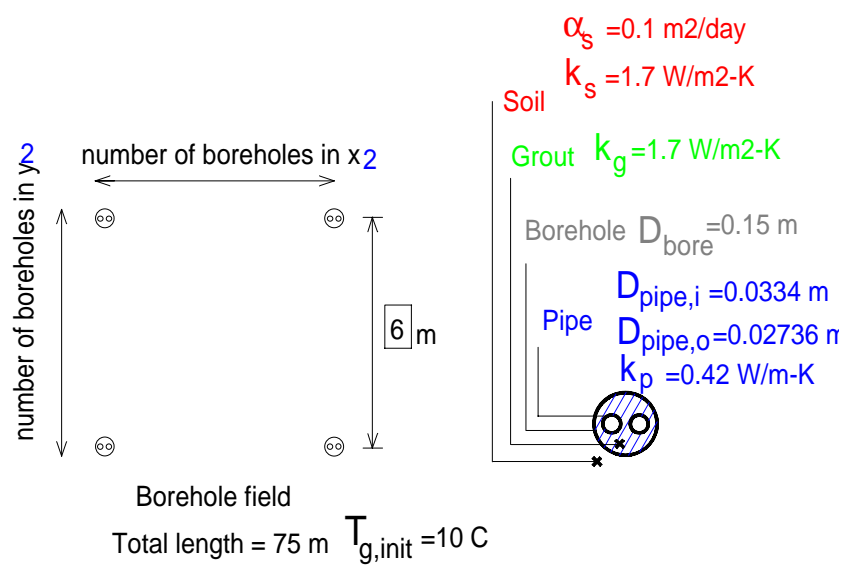


Figure 5. Input screen for borefield and for the ground/bore properties.

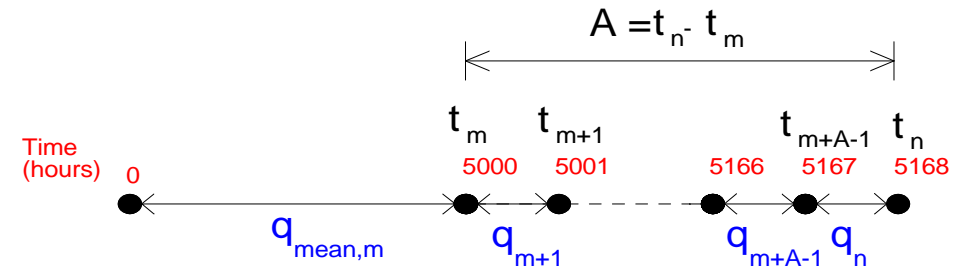


Figure 6. Schematic representation of load aggregation

Model_A_cooling			Model_A_heating		
Row	EWT [C]	COP	Row	EWT [C]	COP
Row 1	10	5.31	Row 1	-1.1	2.94
Row 2	15.6	4.78	Row 2	4.4	3.28
Row 3	21.1	4.28	Row 3	10	3.66
Row 4	26.7	3.67	Row 4	15.6	3.98
Row 5	29.4	3.55	Row 5	21.1	4.31
Row 6	32.2	3.36	Row 6	26.7	4.61
Row 7	37.8	2.92	Row 7	32.2	4.84
Row 8	43.3	2.49			

Figure 7. Lookup table to calculate heat pump COP.

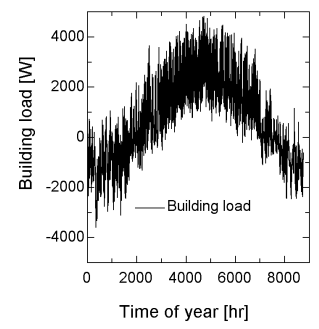


Figure 8. Building load

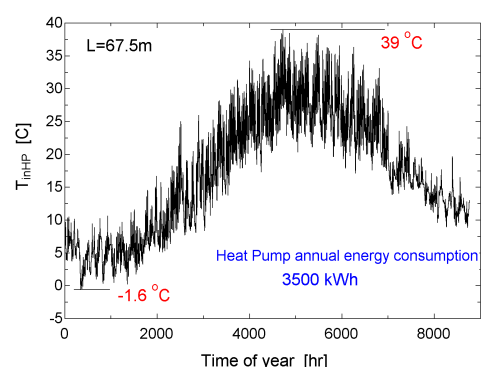
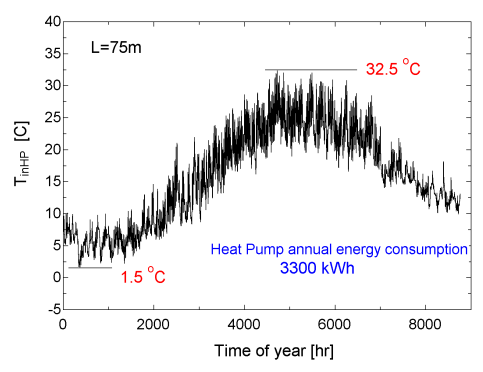


Figure 9. Inlet temperature to the heat pumps for two different heat exchanger lengths.